Surface-Enhanced Raman Spectroscopy Substrates Created *via* Electron Beam Lithography and Nanotransfer Printing

Nahla A. Abu Hatab, Jenny M. Oran, and Michael J. Sepaniak*

Department of Chemistry, University of Tennessee, Knoxville, Tennessee 37996-1600

ABSTRACT The development of quantitative, highly sensitive surface-enhanced Raman spectroscopy (SERS) substrates requires control over size, shape, and position of metal nanoparticles. Despite the fact that SERS has gained the reputation as an information-rich spectroscopy for detection of many classes of analytes, in some isolated instances down to the single molecule detection limit, its future development depends critically on techniques for nanofabrication. Herein, an unconventional nanofabrication approach is used to produce efficient SERS substrates. Metallic nanopatterns of silver disks are transferred from a stamp onto poly(dimethysiloxane) (PDMS) to create nanocomposite substrates with regular periodic morphologies. The stamp with periodic arrays of square, triangular, and elliptical pillars is created via electron beam lithography (EBL) of ma-N 2403 resist. A modified cyclodextrin is thermally evaporated onto the stamp to overcome the adhesive nature of the EBL resist and to function as a releasing layer. Subsequently, Ag is physically vapor deposited onto the stamp at a controlled rate and thickness and used *directly* for nanotransfer printing (nTP). Stamps, substrates, and the efficiency of the nTP process were explored by scanning electron microscopy. Transferred Ag nanodisk—PDMS substrates are studied by SERS using Rhodamine 6G as the probe analyte. There are observed optimal conditions involving both Ag and cyclodextrin thickness. The SERS response of metallic nanodisks of various shapes and sizes on the original stamp is compared to the corresponding nTP created substrates with similar trends observed. Limits of detection for crystal violet and Mitoxantrone are approximately 10^{-8} and 10^{-9} M, respectively. As an innovative feature of this approach, we demonstrate that physical manipulation of the PDMS post-nTP can be used to alter morphology, *e.g.*, to change internanodisk spacing. Additionally, stamps are shown to be reusable after the nTP process, adding the potential to scale-up regular morphology substrates by a stamp-and-repeat methodology.

KEYWORDS: SERS · electron beam lithography · nanotransfer printing · poly(dimethylsiloxane) · metal–polymer nanocomposites · SEM

Over the past two decades, unconventional nanofabrication techniques have become essential to fabricate structures that have nanometer dimensions for research in material science, biology, chemistry, and physics. These techniques have also been applied in manufacturing microelectronics, biological and chemical sensors, and microfluidic devices.[1] Examples of such techniques developed by pioneers in the field are imprinting lithography, step-and-flash imprint lithography, and nanotransfer printing (nTP).[1–3] Some advantages to these methods include flexible patterning capabilities, experimental simplicity, and low cost.[2] Nanotransfer printing is a high-resolution stamping technique that involves transferring material from relief features on a stamp or mold to a substrate.[3–5] Metallic films or nanoparticle substrates are mainly produced by this method. With nTP, the stamp can be either rigid when created with electron beam lithography (EBL) and reactive ion etching (RIE)[3] or an elastomeric stamp prepared by casting a liquid polymer against a rigid master.[2,6] Nanotransfer printing is a fast process, additive in nature (material is only printed in locations where it is needed), and enabled by interfacial chemical reactions when the stamp and substrate are brought into contact. In addition, the technique avoids exposing the substrate to high temperature or/and harsh materials such as organic solvents or basic and acidic solutions.[1] Preparing noble metallic nanodisk substrates by this method has significant potential in surface-enhanced Raman spectroscopy (SERS).

The observation of SERS by molecules in close proximity to roughened metal surfaces has motivated interest in the technique for chemical and biological applications.[7] In the last two decades, SERS has evolved into a very sensitive spectroscopic technique, providing single molecule sensitivity with enhancement factors as high as 10^{12}–10^{15} in highly specialized cases.[8–13] In addition, SERS spectra provide detailed structural information and high selectivity.[14,15] Despite all of these advantages, SERS has limitations in analytical figures of merit, such as reproducibility and dynamic range. The mechanism of SERS enhancement continues to be an active research topic. However, two mechanisms are well discussed in the literature.[12,16–19] The more general mechanism is based on an electromagnetic effect wherein the local

*Address correspondence to msepaniak@utk.edu.

Received for review November 5, 2007 and accepted December 18, 2007.

Published online January 12, 2008.
10.1021/nn7003487 CCC: $40.75

electromagnetic field at or near laser irradiated noble metal particle surfaces is enhanced as a result of localized surface plasmon excitation leading to more intense Raman scattering from molecules near or adsorbed onto the particle surfaces.[20,21] The electromagnetic mechanism renders SERS intensities strongly sensitive to surface structure, particle size, shape, composition, spatial arrangement, and dielectric environment.[22] The other mechanism is a chemical effect which involves specific interactions or coupling between analyte molecules and the metal particles.[23]

Over the years, several different techniques have been developed to create or fabricate functional noble-metal SERS substrates. The most commonly used substrates are disorganized media such as metal colloidal films,[24,25] metal-island films on glass,[26–28] electrochemically roughened silver electrodes,[29,30] or polymer nanoparticle surfaces.[31,32] However, limitations in all these techniques include the complexity of these irregular surfaces, reproducibility from one experiment to another, and heterogeneity of the surface, which make elucidating details of the mechanisms of SERS a difficult task. Recent research has led to the preparation of metal particles with tunable shapes and sizes using chemical reactions in solution—wet chemistry such as rods,[33–35] cubes,[36,37] and disks.[38] Another method to prepare more uniform and controllable SERS substrates is nanosphere lithography, where regular structures with truncated tetrahedral shapes are produced.[39] Among the lithographic techniques, EBL with RIE allow for the optimization of the periodic structure, shape, and spacing.[40–47] However, EBL techniques are associated with high preparation cost and scale-up issues.

Previous studies in our research group showed interesting SERS responses for a direct EBL technique where densely packed polymeric arrays of pillars with different shape, spacing, and arrangements were fabricated and metallized *via* physical vapor deposition to create metal nanodisks on top of the pillars.[48] Here, for the first time we have used nTP to transfer Ag patterns from the resist stamp onto an elastomer poly(dimethylsiloxane) (PDMS) substrate to fabricate reproducible, uniform ordered arrays of metallic nanostructures for SERS research. The motivation for this approach is to increase the density of components, scale up production, and improve cost effectiveness and performance. The flexibility of this nanofabrication technique enables the rapid generation of several substrates that contain patterns with a variety of geometries. Thus, we can rapidly examine a fairly large number of substrate designs for SERS. In this work the most efficient EBL stamps for nTP can be obtained by coating the stamp with heptakis(6-*O*-*tert*-butyldimethylsilyl-2,3-di-*O*-acetyl)-β-cyclodextrin (H-β-CD) as a metal-releasing phase. The capability to transfer isolated metal nanodisks is verified with scanning electron microscopy (SEM). The SERS response of metallic nanodisks of various shapes and sizes

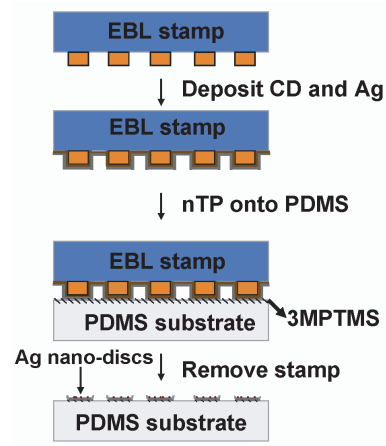

Figure 1. Schematic illustration of procedures for using nTP to fabricate nanodisk SERS substrates.

on the original stamp is compared to the corresponding nTP created substrates, with similar trends observed. Specifically, by using the nTP technique and PDMS as a pliable substrate that can be physically manipulated, one can alter the gaps between the transferred Ag nanodisks. Moreover, by stamping and repeating, several SERS-active substrates or greater area can be produced using the same EBL-fabricated stamp.

RESULTS AND DISCUSSION

Description of the Technique. Nanotransfer printing involves four different components or operations: a stamp which can be rigid or elastomeric with relief features of the desired pattern, a technique or method to deposit a thin film of material onto the raised features of the stamp, a means of bringing the stamp into physical contact

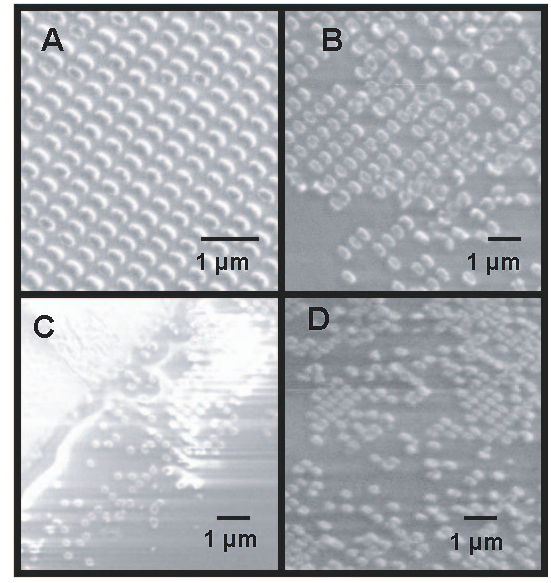

Figure 2. Scanning electron micrographs of the E63_1 pattern: (A) nanodisk arrays transferred from a stamp under optimal conditions, 50 nm of H-β-CD followed by 50 nm of Ag; (B–D) nanodisk arrays transferred from a stamp under nonoptimal conditions, (B) 50 nm of Cal-4 followed by 50 nm of Ag, (C) 20 nm of H-β-CD followed by 50 nm of Ag, (D) 50 nm of H-β-CD followed by 20 nm of Ag.

with the substrate, and in many cases a surface chemistry to prevent adhesion of deposited material to the stamp and promote its adhesion to the substrate.[1,2] The rigid stamp is often fabricated by pattering an e-beam resist on a Si substrate and etching the exposed regions of the substrate with an anisotropic reactive ion etch, then removing the resist.[2] Here, in contrast with usual nTP approaches to fabricate nanometal arrays,[3–5] our method is simply based on *direct* use of the EBL stamp without any further processes. After preparation of the stamp using ma-N 2403 negative photoresist and EBL, H-β-CD is thermally evaporated onto the stamp to function as a releasing layer. This is necessary because the resist used here to create the pillars is a methacrylate-based negative e-beam resist and, as with most, is characterized as being an adhesive polymer.[49,50] Subsequent to the formation of a releasing layer, the stamp is metallized with Ag (the most common SERS metal) *via* physical vapor deposition to create isolated metal nanoparticles (nanodisks). These isolated metal nanodisks are transferred onto PDMS to create nanocomposite substrates with regular periodic morphologies. Placing the metal-coated stamp on top of PDMS with minimum applied pressure leads to close, conformal contact between the raised regions of the stamp and the PDMS substrate. Peeling the substrate and stamp apart transfers the Ag from the raised regions of the stamp to the substrate. The transferring process relies on a common condensation reaction and self-assembled monolayer chemistry.[4] This technique enables successful metallic transferring without the need to combine EBL with any other techniques.[3] A schematic drawing of the fabrication process is shown in Figure 1 and the nanodisk shapes and dimensions are provided in Table 1.

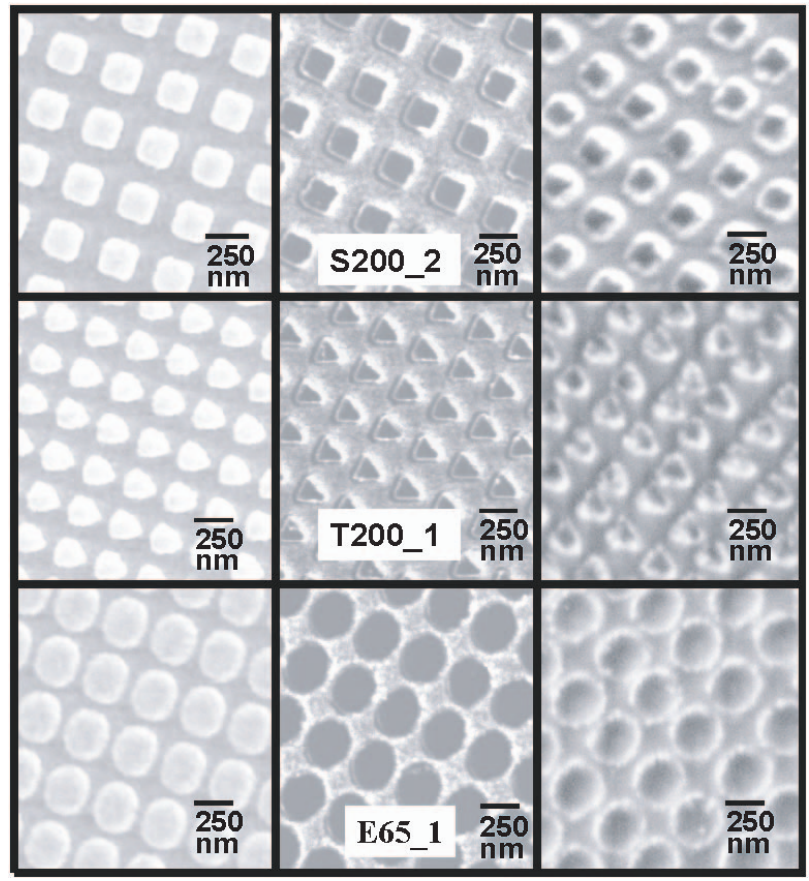

Figure 3. Scanning electron micrographs of a 50 nm H-β-CD followed by 50 nm thick Ag evaporated on the stamp (left column), stamp after nTP (middle column), and PDMS substrates showing integrity of the nanotransfer printing (right column). All micrographs were collected at a 15k magnification.

TABLE 1. EBL-Created Patterns and Dimensions

Pattern	L (nm)	W (nm)	H (nm)	Gap (nm)	Shape
S200_1	200	200	50	100	
S200_2	200	200	50	200	
S300_1	300	300	50	100	
S300_2	300	300	50	200	
E63_1	300	150	50	100	
E63_2	300	150	50	200	
E65_1	300	250	50	100	
E65_2	300	250	50	200	
T100_1	100	100	50	100	
T200_1	200	200	50	100	

Optimization and Performance. Parameters that were optimized for the nTP process include the following: type of the phase used to cover the resist and behave as a releasing layer for Ag, thickness of the phase, and thickness of Ag. Transfer pressure was found not to be critical in our work since the elasticity and mechanical properties of the PDMS substrate ensure close contact at the stamp/substrate interface with minimum pressure being applied. All studies presented here were done with roughly 75 g/cm^2 contact pressure. The first step was to test and compare the releasing efficacy of different phases such as H-β-CD and 4-*tert*-butylcalix[4]arene (Cal-4). Panels A and B of Figure 2 represent SEM images of the transferred nanodiscs using layers of 50 nm H-β-CD and 50 nm Cal-4 releasing phases, respectively. These results show that the H-β-CD phase, which had been synthesized for molecu-

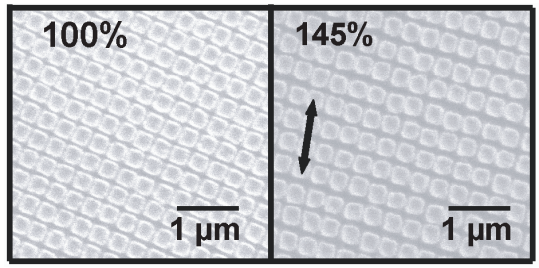

Figure 4. Scanning electron micrographs of the S200_1 nanodisk arrays transferred from a stamp and after being stretched. The arrow denotes the stretching direction.

lar recognition in sensing,[51] is more efficient for the nTP process than simple Cal-4. This may be a result of the greater hydrophobic nature of the cyclodextrin and weaker adhesion to metal or its ability to break apart during the transfer process. The effect of the thickness of H-β-CD phase for the nTP process was investigated. Thicknesses of 20, 35, and 50 nm were deposited on three separate EBL stamps, and Ag thickness was kept constant at 50 nm. SEM images showed that the best performance for the nTP process is yielded when the thickest, 50 nm, H-β-CD phase is applied (compare Figure 2A with Figure 2C). This amount seems to be large for a releasing layer, which may be an indication that the e-beam resist and H-β-CD create a mixed layer before a distinct layer of the CD is eventually formed. Although an extensive investigation was not conducted, it is likely that numerous compatible phases with properties such as this particular cyclodextrin can be found.

Ag was deposited on the EBL stamp at thicknesses of 20, 35, and 50 nm. In each case stamps were first coated with 50 nm H-β-CD phase. Upon the nTP process, SEM images showed that 50 nm of Ag gave the most promising results with minimum defects in the nTP process. Figure 2D shows the PDMS substrate with minimum numbers of nanodisks being transferred when only 20 nm of Ag was deposited. With further study, conditions to create nanodisks of a range of thicknesses and releasing coating phases would be beneficial.

For three different patterns, Figure 3 shows SEM images of the stamp after the deposition of 50 nm of H-β-CD and 50 nm of Ag (left column). Similarly, SEM images of the stamp after the nTP process and the PDMS substrate with the transferred Ag nanodisks are shown in the middle column and the right column, respectively. It can be seen that the Ag that is vapor deposited in the interstices between the pillars is not transferred and only the nanodisks are printed. The appearance of a contrast at the edges of the nanodisks is probably an indication that a portion of the Ag on the sides of the e-beam pillars is also transferred. Low-resolution SEMs (not shown) indicate that the entire 40 × 40 μM EBL pattern is transferred as shown in Figure 3.

Altering the space or the gap between nanometallic particles has shown in experimental studies to have significant impact on optical properties and SERS signal[7,42,52] and in modeling work predicted to have very dramatic effects.[19,53,54] With EBL alone, resolution is limited by the electron beam and the resist properties and may not permit closing the gap adequately to produce extremely hot (high field) spots between nanoparticles. Conversely, combining EBL and nTP provides the unique capability to alter the morphology and the interparticle gap of the Ag nanodisks by stretching and relaxing the PDMS substrate. In this way, substrates with the structural dimensions required for optimum SERS enhancement may be attainable. A preliminary result for this is shown in Figure 4 where after the nTP process, the PDMS substrate was mechanically stretched slowly (in one direction) up to 145% of the original post-cured length. The micrographs in the figure indicate that gaps between nanodisks are in proportion to the degree of stretch; thus surface morphology can be controlled by nTP onto pliable PDMS substrates. The approach to close the gap would be to nTP onto stretched polymer and then relax. PDMS is one of the most common elastomers for research and in our studies has been stretched and relaxed over the range 100−150%. However, polymers such as Kraton G, polystyrene poly(ethylene-butylene)polystyrene, can be manipulated several fold in dimensional changes without rupture.[55,56]

SERS Response and Comparison Studies. In the past, our group has demonstrated the potential advantages of using metal–polymer nanocomposites as random morphology substrates for SERS.[57] Moreover, we have further exploited the advantages of EBL to create nanostructured polymer (e-beam resist) surfaces with a variety of shapes, sizes, and orientations.[48] Herein, we evaluated the performance of nTP-based SERS sub-

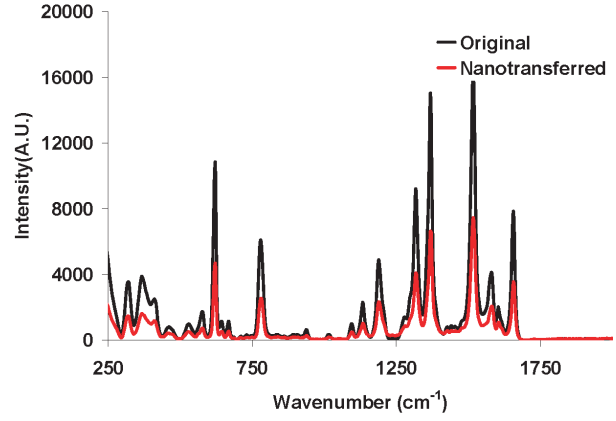

Figure 5. Comparison of R6G (1 × 10^{-6} M) SERS spectra for E63_1 pattern from a stamp (50 nm Ag disks) (black) and upon nTP of the nanodisk array onto PDMS (red).

strates and compared them to the original EBL nanodisks. One should note that the thicknesses of the Ag nanodisk surfaces used herein are greater than the optimum thickness for silver island on smooth glass ~8 nm, silver deposited on PDMS ~18.5 nm,[57] and silver deposited in our prior work on EBL nanodisks ~20 nm.[48] The optimum thickness for regular periodic nanodisks will depend, however, on the other dimensions, dielectric properties of the medium, and the excitation wavelength.

Figure 5 shows Rhodamine 6G (R6G) spectra of the original and nanotransferred E63_1 Ag disks. One possible explanation for the modest drop in the signal in the figure is that some of the H-β-CD is probably transferred with the Ag nanodisks, thus influencing dielectric properties and the partitioning of the R6G onto the Ag surface. Different disk shapes (squares, ellipses, and triangles), dimensions, and gap sizes were compared using the magnitude of the R6G SERS band area centered at 767 cm^{-1}. The results for this comparison study are shown in Figure 6. Each bar in these graphs corresponds to the average of 16 data points within a given array and the average of three different arrays of a given pattern. For the square disks (Figure 6A), the original disks, and nTP disks, SERS responses are following the same trend.

Previous studies in our group have shown that arrays of elliptical nanodisks have interesting SERS results.[48,58] To examine their performance for the nTP process, we fabricated close-packed arrays of these disks with two lateral dimensions 300:250 nm and 300:150 nm (long axis:short axis). The gaps were changed from 100 to 200 nm for each pattern. The results in Figure 6B show an increase in the R6G SERS signal when the lateral dimensions change from 300:150 nm to 300:250 nm and the gap decreases from 200 to 100 nm. These results are consistent with our previous data and calculations.[58] Both the elliptical and triangular patterns compared well in terms of trends (original *vs* nTP based signals). However, as with the smaller 100 nm squares, the smaller 100 nm triangles did not develop well in the EBL stage. Considering that each step in the nanodisk preparation protocol (EBL, vapor depositions, actual nTP) can be expected to distort the structures originally computationally created, it is reassuring that reasonably good consistency in SERS response trends is observed. We have acquired optical extinction spectra in previous work as an additional means of optical characterization.[57,59] However, the small sizes of our patterns make the acquisition of optical extinction spectra somewhat difficult, and since we were able to demonstrate the integrity of the nTP process with SEM and SERS experiments, no attempt was made to acquire such spectra.

The EBL approach can be used to create regular arrays of many different morphologies,[48] but the main disadvantage of EBL is the high operational cost, particularly when creating large areas of substrate. As a result, nTP can be the basis for economical nanofabrication of SERS substrates when the same EBL stamp can be reused multiple times to create extended nanodisk arrays. SERS responses were investigated for the first, second, and third nTP using the same stamp by collecting the spectra for R6G each printing of the T200_1 pattern (see Figure 7). The RSD for the average SERS band area of the 767 cm^{-1} band of 1×10^{-6} M R6G was determined to be 13% for the spectra in the figure. Thus, we have demonstrated for the first time an ability to use a stamp-and-repeat protocol to address the scaling limitation in creating EBL-based SERS substrates.

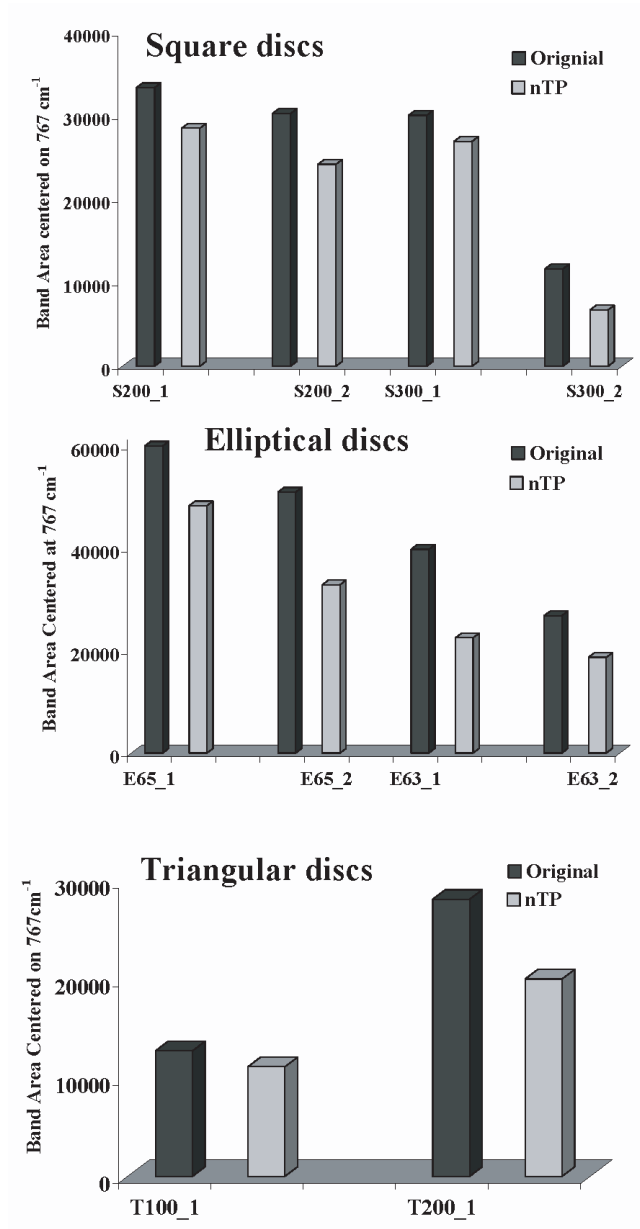

Figure 6. Comparison of the 767 cm^{-1} band area SERS signal of R6G (1×10^{-6} M) for stamp and nTP substrate as a function of the geometric pattern.

Sensitivity is an important figure of merit for SERS. Herein, the nTP substrates were tested for sensitivity

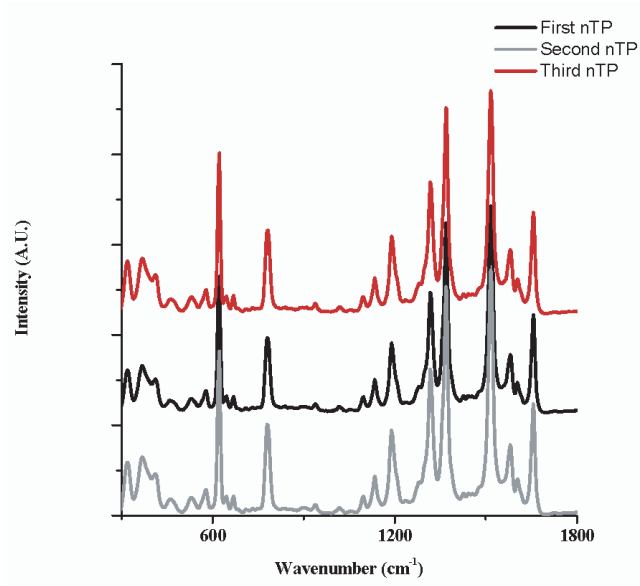

Figure 7. SERS spectra of R6G (1×10^{-6} M) using the same nanodisk stamp nTP onto three different PDMS substrates.

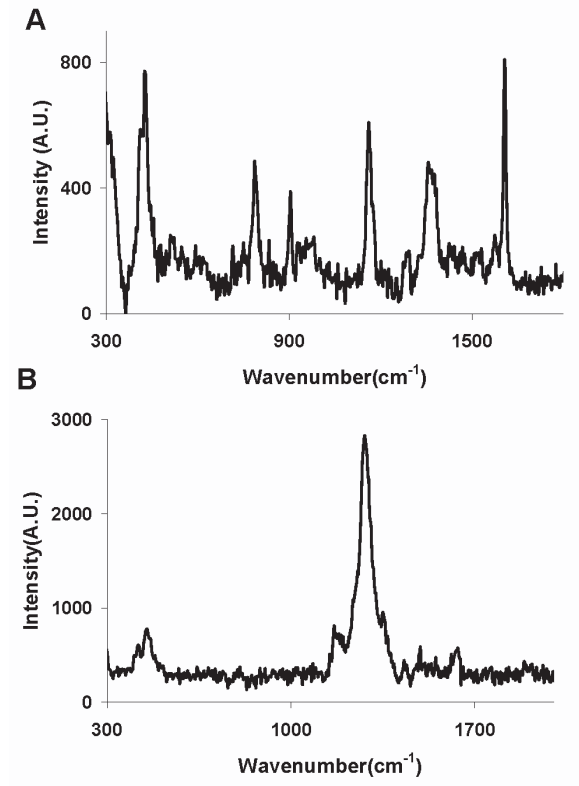

Figure 8. Spectra of crystal violet (A) and Mitoxantrone (B) at 10^{-8} and 10^{-9} M, respectively.

by obtaining spectra near the detection limit for crystal violet dye (nonresonant SERS case) and for Mitoxantrone (absorption maximum at ~650 nm[60] rendering this a resonance SERS case). Figure 8 shows the spectra of 1×10^{-8} M crystal violet and 1×10^{-9} M Mitoxantrone that demonstrate good sensitivity for these analytes using the nTP-created substrates. In our previous work using Ag colloid SERS substrates and these analytes,[59] the drug Mitoxantrone yielded about 3 orders of magnitude better detectability than crystal violet. We attribute this change in apparent selectivity to the dual function of the H-β-CD. Specifically, it acts both as a releasing agent and as a metal overcoating layer that exhibits molecular recognition properties which influence the partitioning of the analytes to the metal surface.

CONCLUSIONS

In summary, we have studied and characterized the performance of Ag nanodisk patterns developed by EBL and nTP. Using physical vapor deposition to coat the EBL nanopillars with H-β-CD to overcome the adhesive nature of ma-N 2403 resist proved to be effective and efficient. It is observed that there are optimum conditions for the nTP process such as thickness and type of the releasing phase. With this cost-effective approach, mechanical or physical manipulation of the pliable PDMS substrates allows for control of the gaps between metallic nanostructures with intriguing implications for creating highly performing SERS substrates. Although the SERS signal of the nTP nanodisks is seen to be slightly lower than the signal of the original EBL nanodisks, they follow similar trends as disk shapes and dimensions are changed. Overall, the SERS signal of the transferred silver nanoparticles onto the PDMS substrate demonstrate nTP as a promising nanofabrication method to overcome the drawback of the high cost of EBL and to fabricate extended structures as SERS substrates.

MATERIALS AND METHODS

Surface-Enhanced Raman Spectroscopy Instrumentation. The SERS spectra were acquired using a LabRam spectrograph from JY-Horiba. The instrument setup has been described in detail previously.[61] In general, the instrument uses an Olympus BX-40 microscope with a 10× (0.25 NA, ∞) objective that delivers up to 9 mW of the 632.8 nm line from an electrically cooled He−Ne laser. The laser spot size in these studies was approximately 20–25 μm. All spectra were acquired in a 180° scattering geometry with a 2936 cm^{-1} spectral window. In this work, all sample acquisition times were set to 1 s.

Preparation of the Stamp Substrates. A set of two-dimensional models of squares, triangles, and elliptical nanoarrays were designed in AutoCAD 2005. Pattern size varies between 100 and 300 nm in the lateral dimension with an interparticle spacing of 100 or 200 nm (see Table 1 for details). Following that, each drawing was converted to GDS-II format by using the LinkCAD conversion program. The files were transferred and programmed into the EBL computer. A 300 nm film of ma-N 2403, a methacrylate-based negative e-beam resist, was uniformly applied to the surface of a new 2 in. wafer (Wafer World, West Palm Beach, FL) by spin coating at 3000 rpm for 30 s. The coated wafer was then baked at 90 °C in a conventional oven for 60 s and placed into the EBL system. Film thickness of the ma-N 2403 re-

sist was estimated from a chart provided by the manufacturer and is based on spin rate.

A Jeol JBX-6000 FS/E electron beam lithography system with a 50 keV thermal-field-emission gun was used for the nanofabrication of the stamp. The ma-N 2403 resist film was exposed to a beam of 170 $\mu C/cm^2$, yielding an array of nanopatterns. Each array is approximately 40 $\times$ 40 μm in size with 500 μm spacing in the *x* direction and 100 μm spacing in the *y* direction between each uniquely patterned array. Once exposed, the ma-N 2403 patterns were developed in alkaline ma-D 332 developer for 6 s and rinsed in deionized water (18 MΩ, Barnstead E-Pure) for 3 min. After development, the ma-N 2403 patterns were carefully dried using a low-flow stream of N_2 gas.

The stamps were then prepared for nanotransfer printing as follows by first using an in-house made physical vapor deposition system to vapor deposit H-β-CD and Cal-4. This system uses a light source for heating and operates at roughly 10^{-2} Torr. Average mass thickness and deposition rates were measured for each film with a Maxtec quartz-crystal microbalance that is mounted adjacent to the arrays. Details on this procedure can be found in prior reports.[62–64] A physical vapor deposition chamber from Cooke Vacuum Products, Inc., was then used to vapor deposit Ag. Samples were mounted 25 cm above and normal to the effusive source. The ma-N 2403 arrays were first coated with different thickness of H-β-CD (the CD was prepared using the method of Stoddart *et al.*[65]) and Cal-4 (Lancaster, Pelham, NH). Next the arrays were coated with 50 nm of 99.99% Ag (Alfa Aesar, MA) under high vacuum conditions (1×10^{-6} Torr). Once prepared, stamps were stored in a vacuum desiccator in the dark prior to use (see Table 1 for substrate specifications). To reuse the stamp, traces of Ag were etched out by placing the stamp in an aqueous solution of 0.2% w/v $HAuCl_4$ for 6 min. The stamp was then rinsed with copious amount of water after etching. After the stamp was dried, 20 nm of H- β-CD was deposited followed by 50 nm of Ag and the stamp was reused for nTP.

Preparation of the SERS Substrate. A 2 in. Si wafer was cleaned with ethanol (HPLC, Fisher). PDMS was prepared by the addition of Sylgard 184 curing agent (Dow Corning) and its elastomer in a 1:10 mass to mass ratio. The two compounds were combined and then degassed under high vacuum for 15 min. PDMS was spin coated at 200 rpm for 30 s, and then cured in the oven at 70 °C for 1 h to create the film. PDMS was stored at room temperature until completely cured. The PDMS film was peeled off the wafer, and the side facing the Si wafer was treated with UV−ozone for 3 min in a UVO cleaner (Jelight Co., Inc., Irvine, CA). It was then treated with 1×10^{-5} M (3-mercaptopropyl)trimethoxysilane (3MPTMS, 95%, Aldrich, with acetone as the solvent) for 24 h. Following that, the PDMS film was rinsed with deionized water (18 MΩ, Barnstead E-Pure) for 1 min. The stamps were placed on top of the treated PDMS under a metal block that provided roughly 75 g/cm^2 pressure and left in a vacuum desiccator held at 10^{-4} Torr in the dark for 1 h to transfer the patterns.

All SEM images were collected using a LEO 1525 scanning electron microscope with a field-emission gun operating at 22 kV, 2 kV for the stamp and PDMS, respectively. Images were obtained in secondary electron detection mode. These operating conditions were applied to reduce the sample damage and the buildup of charge while producing high-resolution images of stamp and the PDMS substrate surfaces.

Sample Preparation. The test analyte solutions used in these studies were 1×10^{-6} M Rhodamine 6G (98+%, Allied Chemicals), 1×10^{-8} M crystal violet (Fisher), and 1×10^{-9} M Mitoxantrone dihydrochloride (sigma), and all were prepared in deionized water (18 MΩ, Barnstead E-Pure).

Data Acquisition and Analysis. The substrates were placed at the bottom of a plastic Petri dish, filled with a 2 mL aliquot of each sample solution. The maximum SERS signal was obtained by fine-focusing the microscope objective of the Raman spectrometer, and the spectroscopic data were collected by moving the stage at 10 μm intervals (1 spectral acquisition per step) over a 1600 μm^2 area. All Ag substrates were irradiated with 4.1 mW of the 632.8 nm line of a He−Ne laser for 1 s. Average spectra were collected on three arrays of the same pattern. The average of these spectra for each pattern was used for the interpretation of the analytical data. For the elliptical nanodisk arrays, spectra were collected with the polarization vector of the laser being parallel to the long axis of the disk.

Acknowledgment. This work was supported by the U.S. Environmental Protection Agency STAR Program under Grant EPA-83274001. Support for this work was also provided *via* a grant from the Oak Ridge National Laboratory, Center for Nanophase Material Science (CNMS). The authors thank Dr. Mustafa Culha for synthesizing the modified cyclodextrin and Dr. Scott Retterer of CNMS and Dr. David Joy of UTK for assistance with EBL.

REFERENCES AND NOTES

1. Gates, B. D.; Xu, Q.; Stewart, M.; Ryan, D.; Willson, C. G.; Whitesides, G. M. New Approaches to Nanofabrication: Molding, Printing, and Other Techniques. *Chem. Rev.* **2005**, *105*, 1171–1196.
2. Menard, E.; Rogers, J. A. Stamping Techniques for Micro- and Nanofabrication. *Springer Handbook of Nanotechnology*, 2nd ed.; Springer: Berlin, 2007; pp 279−297.
3. Loo, Y.-L.; Willett, R. L.; Baldwin, K. W.; Rogers, J. A. Additive, Nanoscale Patterning of Metal Film with a Stamp and a Surface Chemistry Mediated Transfer Process: Applications in Plastic Electronics. *Appl. Phys. Lett.* **2002**, *81*, 562–564.
4. Loo, Y.-L.; Willett, R. L.; Baldwin, K. W.; Rogers, J. A. Interfacial Chemistries for Nanoscale Transfer Printing. *J. Am. Chem. Soc.* **2002**, *124*, 7654–7655.
5. Loo, Y.-L.; Hsu, J. W. P.; Willett, R. L.; Baldwin, K. W.; West, K. W.; Rogers, J. A. High-Resolution Transfer Printing on Gas Surfaces Using Alkane Dithiol Monolayers. *J. Vac. Sci. Technol., B* **2002**, *20*, 2853–2856.
6. Lee, B. H.; Cho, Y. H.; Lee, H.; Lee; K, D.; Kim, S. H.; Sung, M. M. High-Resolution Patterning of Aluminum Thin Film with a Water-Mediated Transfer Pprocess. *Adv. Mater.* **2007**, *19*, 1714–1718.
7. Dieringer, J. A.; McFarland, A. D.; Shah, N. C.; Stuart, D. A.; Whitney, A. V.; Yonzon, C. R.; Young, M. A.; Zhang, X.; Van Duyne, R. P. Surface Enhanced Raman Spectroscopy: New Materials, Concepts, Characterization Tools, and Applications. *Faraday Discuss.* **2006**, *132*, 9–26.
8. Bizzarri, A. R.; Cannistraro, S. Temporal Fluctuations in Single-Molecule SERS Spectra. *Top. Appl. Phys.* **2006**, *103*, 279–296.
9. Chen, K.; Vo-Dinh, T. Single-Molecule Detection Techniques for Monitoring Cellular Activity at the Nanoscale Level. *Nanotechnol. Biol. Med.* **2007**, 16/1–16/24.
10. Habuchi, S.; Hofkens, J. Single-Molecule Surface-Enhanced Resonance Raman Spectroscopy of the Enhanced Green Fluorescent Protein EGFP. *Top. Appl. Phys.* **2006**, *103*, 297–312.
11. Kneipp, H.; Kneipp, K. Surface-Enhanced Hyper Raman Scattering in Silver Colloidal Solutions. *J. Raman Spectrosc.* **2005**, *36*, 551–554.
12. Kneipp, K.; Kneipp, H. Single Molecule Raman Scattering. *Appl. Spectrosc.* **2006**, *60*, 322A.
13. Otto, A. What is Observed in Single Molecule SERS, and Why. *J. Raman Spectrosc.* **2002**, *33*, 593–598.
14. Vo-Dinh, T.; Allain, L. R.; Stokes, D. L. Cancer Gene Detection Using Surface-Enhanced Raman Scattering (SERS). *J. Raman Spectrosc.* **2002**, *33*, 511–516.
15. Zhang, X.; Shah, N. C.; Van Duyne, R. P. Sensitive and Selective Chem/Bio Sensing Based on Surface-Enhanced Raman Spectroscopy (SERS). *Vib. Spectrosc.* **2006**, *42*, 2–8.
16. Kneipp, K.; Kneipp, H.; Bohr, H. G. Single-Molecule SERS spectroscopy. *Top. Appl. Phys.* **2006**, *103*, 261–278.
17. Haynes, C. L.; Yonzon, C. R.; Zhang, X.; Van Duyne, R. P. Surface-Enhanced Raman Sensors: Early History and the Development of Sensors for Quantitative Biowarfare Agent and Glucose Detection. *J. Raman Spectrosc.* **2005**, *36*, 471–484.
18. Moskovits, M.; Tay, L.-L.; Yang, J.; Haslett, T. SERS and the Single Molecule. *Top. Appl. Phys.* **2002**, *82*, 215–226.

19. Schatz, G. C.; Young, M. A.; Van Duyne, R. P. Electromagnetic Mechanism of SERS. *Top. Appl. Phys.* **2006**, *103*, 19–46.
20. Moskovits, M. Surface-Enhanced Raman Spectroscopy. A Brief Perspective. *Top. Appl. Phys.* **2006**, *103*, 1–18.
21. Zou, S.; Schatz, G. C. Coupled Plasmonic Plasmon/Photonic Resonance Effects in SERS. *Top. Appl. Phys.* **2006**, *103*, 67–86.
22. Zhang, X.; Yonzon, C. R.; Young, M. A.; Stuart, D. A.; Van Duyne, R. P. Surface-Enhanced Raman Spectroscopy Biosensors: Excitation Spectroscopy for Optimisation of Substrates Fabricated by Nanosphere Lithography. *IEE Proc.: Nanobiotechnol.* **2005**, *152*, 195–206.
23. Kneipp, K.; Kneipp, H. Surface-Enhanced Raman Scattering on Silver Nanoparticles in Different Aggregation Stages. *Isr. J. Chem.* **2006**, *46*, 299–305.
24. Musick, M. D.; Keating, C. D.; Lyon, L. A.; Botsko, S. L.; Pena, D. J.; Hollay, W. D.; McEvoy, T. M.; Richardson, J. N.; Natan, M. J. Metal Films Prepared by Stepwise Assembly. 2. Construction and Characterization of Colloidal Au and Ag Multilayers. *Chem. Mater.* **2000**, *12*, 2869–2881.
25. Park, S.-H.; Im, J.-H.; Im, J.-W.; Chun, B.-H.; Kim, J.-H. Adsorption Kinetics of Au and Ag Nanoparticles on Functionalized Glass Surfaces. *Microchem. J.* **1999**, *63*, 71–91.
26. Lacy, W. B.; Olson, L. G.; Harris, J. M. Quantitative SERS Measurements on Dielectric-Overcoated Silver-Island Films by Solution-Deposition Control of Surface Concentrations. *Anal. Chem.* **1999**, *71*, 2564–2570.
27. Mulvaney, S. P.; He, L.; Natan, M. J.; Keating, C. D. Three-Layer Substrates for Surface-Enhanced Raman Scattering: Preparation and Preliminary Evaluation. *J. Raman Spectrosc.* **2003**, *34*, 163–171.
28. Reilly, T. H., III; Corbman, J. D.; Rowlen, K. L. Vapor Deposition Method for Sensitivity Studies on Engineered Surface-Enhanced Raman Scattering-Active Substrates. *Anal. Chem.* **2007**, *79*, 5078–5081.
29. Li, J.; Fang, Y. An Investigation of the Surface Enhanced Raman Scattering (SERS) from a New Substrate of Silver-Modified Silver Electrode by Magnetron Sputtering. *Spectrochim. Acta, Part A* **2007**, *66A*, 994–1000.
30. Murgida, D.; Hildebrandt, P. Surface-Enhanced Vibrational Spectroelectrochemistry: Electric Field Effects on Redox and Redox-Coupled Processes of Heme Proteins. *Top. Appl. Phys.* **2006**, *103*, 313–334.
31. Pristinski, D.; Tan, S.; Erol, M.; Du, H.; Sukhishvili, S. In Situ SERS Study of Rhodamine 6g Adsorbed on Individually Immobilized Ag Nanoparticles. *J. Raman Spectrosc.* **2006**, *37*, 762–770.
32. Qian, X. M.; Ansari, D.; Nie, S. A New Class of Nontoxic Nanoparticle Tags Based on Surface Enhanced Raman Scattering. *Proc. SPIE-Int. Soc. Opt. Eng.* **2007**, *6448*, 1–12.
33. Orendorff, C. J.; Gearheart, L.; Jana, N. R.; Murphy, C. J. Aspect Ratio Dependence on Surface Enhanced Raman Scattering Using Silver and Gold Nanorod Substrates. *Phys. Chem. Chem. Phys.* **2006**, *8*, 165–170.
34. Yang, Y.; Xiong, L.; Shi, J.; Nogami, M. Aligned Silver Nnanorod Arrays for Surface-Enhanced Raman Scattering. *Nanotechnology* **2006**, *17*, 2670–2674.
35. White, D. J.; Mazzolini, A. P.; Stoddart, P. R. Fabrication of a Range of SERS Substrates on Nanostructured Multicore Optical Fibres. *J. Raman Spectrosc.* **2007**, *38*, 377–382.
36. Tian, Z.-Q.; Yang, Z.-L.; Ren, B.; Li, J.-F.; Zhang, Y.; Lin, X.-F.; Hu, J.-W.; Wu, D.-Y. Surface-Enhanced Raman Scattering from Transition Metals with Special Surface Morphology and Nanoparticle Shape. *Faraday Discuss.* **2006**, *132*, 159–170.
37. McLellan, J. M.; Siekkinen, A.; Chen, J.; Xia, Y. Comparison of the Surface-Enhanced Raman Scattering on Sharp and Truncated Silver Nanocubes. *Chem. Phys. Lett.* **2006**, *427*, 122–126.
38. Lu, L.; Kobayashi, A.; Tawa, K.; Ozaki, Y. Silver Nanoplates with Special Shapes: Controlled Synthesis and Their Surface Plasmon Resonance and Surface-Enhanced Raman Scattering Properties. *Chem. Mater.* **2006**, *18*, 4894–4901.
39. Zhang, X.; Yonzon, C. R.; Van Duyne, R. P. Nanosphere Lithography Fabricated Plasmonic Materials and Their Applications. *J. Mater. Res.* **2006**, *21*, 1083–1092.
40. Kahl, M.; Voges, E. Analysis of Plasmon Resonance and Surface-Enhanced Raman Scattering on Periodic Silver Structures. *Phys. Rev. B* **2000**, *61*, 14078–14088.
41. Kahl, M.; Voges, E.; Kostrewa, S.; Viets, C.; Hill, W. Periodically Structured Metallic Substrates for SERS. *Sens. Actuators, B* **1998**, *B51*, 285–291.
42. Gunnarsson, L.; Bjerneld, E. J.; Xu, H.; Petronis, S.; Kasemo, B.; Kall, M. Interparticle Coupling Effects in Nanofabricated Substrates for Surface-Enhanced Raman Scattering. *Appl. Phys. Lett.* **2001**, *78*, 802–804.
43. Billot, L.; Lamy de la Chapelle, M.; Grimault, A. S.; Vial, A.; Barchiesi, D.; Bijeon, J. L.; Adam, P. M.; Royer, P. Surface Enhanced Raman Scattering on Gold Nanowire Arrays: Evidence of Strong Multipolar Surface Plasmon Resonance Enhancement. *Chem. Phys. Lett.* **2006**, *422*, 303–307.
44. Yu, Q.; Golden, G. Probing the Protein Orientation on Charged Self-Assembled Monolayers on Gold Nanohole Arrays by SERS. *Langmuir* **2007**, *23*, 8659–8662.
45. Sackmann, M.; Bom, S.; Balster, T.; Materny, A. Nanostructured Gold Surfaces as Reproducible Substrates for Surface-Enhanced Raman Spectroscopy. *J. Raman Spectrosc.* **2007**, *38*, 277–282.
46. Haynes, C. L.; McFarland, A. D.; Zhao, L.; Van Duyne, R. P.; Schatz, G. C.; Gunnarsson, L.; Prikulis, J.; Kasemo, B.; Kaell, M. Nanoparticle Optics: The Importance of Radiative Dipole Coupling in Two-Dimensional Nanoparticle Arrays. *J. Phys. Chem. B* **2003**, *107*, 7337–7342.
47. Hicks, E. M.; Zou, S.; Schatz, G. C.; Spears, K. G.; Van Duyne, R. P.; Gunnarsson, L.; Rindzevicius, T.; Kasemo, B.; Kaell, M. Controlling Plasmon Line Shapes Through Diffractive Coupling in Linear Arrays of Cylindrical Nanoparticles Fabricated by Electron Beam Lithography. *Nano Lett.* **2005**, *5*, 1065–1070.
48. De Jesus, M. A.; Giesfeldt, K. S.; Oran, J. M.; Abu-Hatab, N. A.; Lavrik, N. V.; Sepaniak, M. J. Nanofabrication of Densely Packed Metal-Polymer Arrays for Surface-Enhanced Raman Spectrometry. *Appl. Spectrosc.* **2005**, *59*, 1501–1508.
49. Moszner, N.; Salz, U.; Zimmermann, J. Chemical Aspects of Self-Etching Enamel-Dentin Adhesives: A Systematic Review. *Dental Mater.* **2005**, *21*, 895–910.
50. Whitaker, G.; Kincaid, B. J.; Raftery, D. P.; Van Hoof, N.; Regan, F.; Smyth, M. R.; Leonard, R. G. Potential of CE for the Determination of Inorganic and Acidic Anions in Cyanoacrylate Adhesives. *Electrophoresis* **2006**, *27*, 4532–4537.
51. Culha, M.; Schell, F. M.; Fox, S.; Green, T.; Betts, T.; Sepaniak, M. J. Evaluation of Newly Synthesized and Commercially Available Charged Cyclomaltooligosaccharides (cyclodextrins) for Capillary Electrokinetic Chromatography. *Carbohydr. Res.* **2004**, *339*, 241–249.
52. Wang, H.; Levin, C. J.; Halas, N. J. Nanosphere Arrays with Controlled Sub-10-nm Gaps as Surface-Enhanced Raman Spectroscopy Substrates. *J. Am. Chem. Soc.* **2005**, *127*, 14992–14993.
53. Hinde, R. J.; Sepaniak, M. J.; Compton, R. N.; Nordling, J.; Lavrik, N. Surface-Enhanced Resonance Raman Scattering of Adsorbates Under Liquid Nitrogen. *Chem. Phys. Lett.* **2001**, *339*, 167–173.
54. Hao, E.; Schatz, G. C. Electromagnetic Fields Around Silver Nanoparticles and Dimers. *J. Chem. Phys.* **2004**, *120*, 357–366.
55. Jaziri, M.; Kallel, T. K.; Mbarek, S.; Elleuch, B. Morphology Development in Polyethylene/Polystyrene Blends: The Influence of Processing Conditions and Interfacial Modification. *Polym. Int.* **2005**, *54*, 1384–1391.
56. De Groot, H. Recent Developments of KRATON G Polymers for TPE-S Compounds. *TPE 2003, Int. Conf. New Oppor. Thermoplast. Elastomers, 6th* **2003**, 157–169.

57. Giesfeldt, K. S.; Connatser, R. M.; De Jesus, M. A.; Lavrik, N. V.; Dutta, P.; Sepaniak, M. J. Studies of the Optical Properties of Metal-Pliable Polymer Composite Materials. *Appl. Spectrosc.* **2003**, *57*, 1346–1352.
58. Oran, J. M.; Hinde, R. J.; Abu Hatab, N.; Sepaniak, M. J. Nanofabricated Periodic Arrays of Silver Elliptical Discs as SERS Substrates. *Appl. Spectrosc.* **2007**, .
59. Abu-Hatab, N. A.; John, J. F.; Oran, J. M.; Sepaniak, M. J. Multiplexed Microfluidic Surface-Enhanced Raman Spectroscopy. *Appl. Spectrosc.* **2007**, *61*, 1116–1122.
60. Cunningham, D.; Littleford, R. E.; Smith, W. E.; Lundahl, P. J.; Khan, I.; McComb, D. W.; Graham, D.; Laforest, N. Practical Control of SERRS Enhancement. *Faraday Discuss.* **2006**, *132*, 135–145.
61. De Jesus, M. A.; Giesfeldt, K. S.; Sepaniak, M. J. Improving the Analytical Figures of Merit of SERS for the Analysis of Model Environmental Pollutants. *J. Raman Spectrosc.* **2004**, *35* (10), 895–90.
62. Lavrik, N. V.; Tipple, C. A.; Sepaniak, M. J.; Datskos, P. G. Enhanced Chemi-Mechanical Transduction at Nanostructured Interfaces. *Chem. Phys. Lett.* **2001**, *336*, 371–376.
63. Culha, M.; Lavrik, N. V.; Schell, F. M.; Tipple, C. A.; Sepaniak, M. J. Characterization of Volatile, Hydrophobic Cyclodextrin Derivatives as Thin Films for Sensor Applications. *Sens. Actuators, B* **2003**, *B92*, 171–180.
64. Dutta, P.; Senesac, L. R.; Lavrik, N. V.; Datskos, P. G.; Sepaniak, M. J. Response Signatures for Nanostructured, Optically-Probed, Functionalized Microcantilever Sensing Arrays. *Sens. Lett.* **2004**, *2*, 238–245.
65. Rojas, M. T.; Koeniger, R.; Stoddart, J. F.; Kaifer, A. E. Supported Monolayers Containing Preformed Binding Sites. Synthesis and Interfacial Binding Properties of a Thiolated β-Cyclodextrin Derivative. *J. Am. Chem. Soc.* **1995**, *117*, 336–43.